Non-Invasive Assessment and Control of Ultrasound-Mediated Membrane Permeabilization

Jin Liu,[1] Thomas N. Lewis,[2] and Mark R. Prausnitz[1,3]

Received January 13, 1998; accepted March 21, 1998

Purpose. Ultrasound has been shown to transiently permeabilize biological membranes, thereby facilitating delivery of large compounds such as proteins and DNA into cells and across tissues such as skin. In this study, we sought to quantitatively determine the dependence of cell membrane permeabilization on ultrasound parameters and to identify acoustic signals which correlate with observed membrane permeabilization.

Methods. Bovine red blood cells were exposed to ultrasound at 24 kHz over a range of controlled conditions. The degree of membrane permeabilization was measured by release of hemoglobin and was determined as a function of ultrasound parameters and measured acoustic signals.

Results. These studies showed that permeabilization increased with incident ultrasound pressure, increased with total exposure time above a threshold of approximately 100 msec, showed a weak dependence on pulse length with a small maximum at 3 msec, and did not depend on duty cycle under the conditions examined. Using measured acoustic spectra we found that red blood cell membrane permeabilization correlated best with the pressure measured at half the driving frequency (f/2 = 12 kHz) and its ultraharmonics, less strongly with the broadband noise pressure measured between peaks, and least strongly with pressure measured at the driving frequency and its higher harmonics. Permeabilization caused by ultrasound applied at any set of conditions tested in this study could be well predicted by the parameter $\tau \cdot P_{f/2}$, which characterizes the total cavitational exposure.

Conclusions. This study provides a quantitative guide to designing ultrasound protocols useful for drug delivery. The acoustic measurements support the hypothesis that ultrasonic cavitation is the mechanism by which membranes are permeabilized. They also suggest that measurable acoustic signals can provide noninvasive, real-time feedback about membrane permeabilization and drug delivery.

KEY WORDS: cavitation; drug delivery; sonoporation; bovine erythrocyte; hemolysis.

INTRODUCTION

Ultrasound-mediated delivery has potential as a powerful new method for enhancing and targeting administration of drugs, genes, and other therapeutic compounds into and across cells and tissues. Studies have shown that appropriately-applied ultrasound can reversibly permeabilize viable cells so that exogenous material can enter those cells without killing them. This could be useful for targeted delivery of drugs to cells in a specific tissue (e.g., tumor) or for increased uptake of compounds which cross cell membranes poorly (e.g., proteins, DNA). Ultrasound-enhanced delivery to cells has been demonstrated in vitro by uptake of extracellular fluid (1), drugs (2), and DNA into both cells (3–6) and plant tissues (7). Similarly, acoustic effects of lithotripters have been shown to permeabilize cell membranes (8,9). Most recently, dramatically increased transport of small drugs (10,11) and proteins (12,13) has also been shown across skin, of interest for topical and systemic transdermal drug delivery.

Although ultrasound-mediated drug delivery has only recently received increased attention, ultrasound has been a well established diagnostic and therapeutic tool in medicine for decades (14,15). Under conditions which are believed to cause minimal if any effects on cells (i.e., ultrasound at high frequency and low intensity), ultrasonic imaging is in widespread use throughout the world (16). At somewhat greater intensities, therapeutic ultrasound is commonly used to heat tissues for physical therapy and other hyperthermia treatments (17). Under very different conditions (i.e., a spectrum of lower frequencies and high intensity), lithotripsy procedures routinely focus acoustic energy to noninvasively shatter kidney stones so they can be excreted by the body without surgery (18). Kidney stone destruction by lithotripsy is believed to be mediated by cavitation.

Acoustic cavitation involves the creation and oscillation of gas bubbles in a liquid (19). During the low-pressure portion of an ultrasound wave, dissolved gas and vaporized liquid can form gas bubbles. These bubbles then shrink and grow in size, oscillating in response to the subsequent high- and low-pressure portions of the ultrasound wave. This is referred to as stable cavitation. Transient cavitation occurs at greater acoustic pressures, where bubbles violently implode after a few cycles. This implosion can have a number of effects, including transiently raising the local temperature by hundreds of degrees Celsius and the local pressure by hundreds of atmospheres, emitting light by a poorly-understood phenomenon called sonoluminescence, creating short-lived free radicals, and launching a high-velocity liquid microjet.

Cavitation is also believed to be responsible for ultrasonic permeabilization of cells and tissues of interest for pharmaceutical applications (6,11,16). To develop protocols useful for drug delivery, the effects of ultrasound parameters on cavitation and cell membrane permeabilization need to be better established. For that reason, in this study we pursued three goals: (1) quantitatively determine the dependence of red blood cell membrane permeabilization on ultrasound parameters, (2) identify acoustic signals which correlate with observed membrane permeabilization and can thereby be used to provide noninvasive feedback about ultrasound's bioeffects, and (3) use this information for insight into the mechanism by which ultrasound permeabilizes membranes.

EXPERIMENTAL METHODS

Sample Preparation

Freshly drawn bovine blood with Alsevers anticoagulant (Rockland, Gilbertsville, PA) was stored at 4°C for up to 10

[1] School of Chemical Engineering and Institute for Bioengineering and Bioscience, Georgia Institute of Technology, Atlanta, Georgia 30332-0100.

[2] George W. Woodruff School of Mechanical Engineering, Georgia Institute of Technology, Atlanta, Georgia 30332-0405.

[3] To whom correspondence should be addressed. (e-mail: mark.prausnitz@che.gatech.edu)

0724-8741/98/0600-0918$15.00/0

days. Red blood cells were collected by centrifugation (GS-15R, Beckman Instruments, Palo Alto, CA; 400 g, 10 min, 4°C), washed 3 times with phosphate-buffered saline (PBS; pH 7.4; Sigma, St. Louis, MO), and finally suspended in PBS at a red blood cell concentration of 10% by volume. The cell suspension was stored on ice and then gently mixed on a nutator (Innovative Medical Systems, Ivyland, PA) just before use in an experiment.

The cell suspension was added to a sample tube which was prepared by cutting a 15 ml polypropylene centrifuge tube (VWR, Suwanee, GA) at the 4 ml line. After the sample tube was filled with 4 ml of cell suspension, a rubber stopper (VWR) was carefully inserted into the tube to the 3 ml line, thereby spilling out about 1 ml of suspension. This procedure was used so that the tube could be sealed without any entrapped air bubbles. A hydrophone (Baylor School of Medicine, Houston, TX) was also inserted through a small hole in the center of the rubber stopper and positioned at the center of the sample volume.

Exposure to Ultrasound

The ultrasound exposure chamber consisted of a cylindrical piezoelectric transducer (lead zirconate titanate, 5 cm OD, 4.5 cm ID, 2.5 cm length; Channel Industries, Santa Barbara, CA) sandwiched between two 10 cm lengths of 1.5 inch Schedule 40 PVC pipe. The bottom of the chamber was sealed on a clear polycarbonate base (Lexan, General Electric, Mt. Vernon, IN). The chamber was filled with water which was filtered/deionized (Type III; U.S. Filter, Roswell, GA) and degassed (vacuum chamber: Nalgene, Rochester, NY; pump: 2107VA20A, Thomas, Sheboygan, WI).

The sample tube was placed in the water bath within the ultrasound exposure chamber, positioned at the axial and radial center of the transducer, and exposed to low-frequency (24 kHz) ultrasound at room temperature (22 ± 2 °C). A function generator (DS345, Stanford Research Systems, Sunnyvale, CA) was programmed to provide a sinewave of selected voltage, duty cycle, burst length, and total exposure time. The output was fed to an amplifier (Macro-tech 2400, Crown, Elkhart, IN) whose signal went through a matching transformer (MT-56R, Krohn-Hite, Avon, MA) to drive the transducer.

Measurement of Ultrasound Pressure

To monitor the ultrasound exposure, the voltage applied to the transducer was measured with an oscilloscope (54603B, Hewlett Packard, Santa Clara, CA). This voltage was used to estimate the incident ultrasound pressure, as described below. In addition, the signal from the hydrophone in the sample tube was fed to the oscilloscope and a spectrum analyzer (SR760, Stanford Research Systems), which was used to determine the amplitude of different acoustic signals shown in Figure 1 and Table 1.

The strength of ultrasound is reported as its incident pressure. The incident pressure is defined as the pressure level that would exist in the absence of cavitation, which is primarily at the driving frequency (i.e., 24 kHz). This is important because one of the effects of cavitation is to shift acoustic energy to frequencies other than the driving frequency (Figure 1). We believe the incident pressure is the most useful way to characterize ultrasound for this study, because it is independent of apparatus geometry and represents the total relevant acoustic input. For propagating wave fields created by a planar transducer at high frequency, ultrasound strength is often reported as an intensity (e.g., in units W/cm^2). For ultrasonic irradiation of a surface such as skin with a planar transducer (10), this approach makes sense. However, because of the cylindrical geometry of our transducer and the use of low frequency ultrasound with a wavelength comparable to the apparatus diameter, a radially-symmetric standing wave-like field is generated which makes acoustic intensity extremely difficult to determine. Another choice might be to report the pressure directly measured with a hydrophone at the driving frequency. While this is useful at low acoustic levels, where the measured pressure has the same value as the incident pressure, at higher intensities when cavitation occurs acoustic energy is shifted to a spectrum of other frequencies (Figure 1). Thus, the pressure measured at the driving frequency accounts for only a portion of the ultrasound exposure experienced by the cells.

The peak incident pressure generated within the exposure chamber was estimated by measuring the acoustic pressure at subcavitation levels and linearly extrapolating to higher drive levels (20). At supra-cavitation levels, the incident pressure continues to increase as a linear function of the voltage, whereas the measured pressure levels off and may decrease due to cavitation. We therefore generated a linear fit of the data only at low

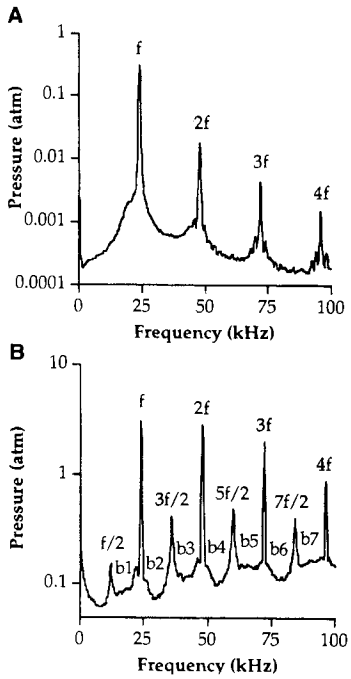

Fig. 1. Representative acoustic spectra measured during ultrasound exposures at (A) low pressure (no cavitation) or (B) high pressure (extensive cavitation). Ultrasound was applied at f = 24 kHz. Due to apparatus resonance and cavitation, higher harmonics of f (e.g., 2f = 48 kHz) are seen under all conditions. Seen only in (B), cavitation also generates other signals: the subharmonic (f/2 = 12 kHz) and its ultraharmonics (e.g., 3f/2 = 36 kHz) and an elevated broadband "noise" level (e.g., b1, b2). The acoustic spectrum measured during exposure of cells to ultrasound can provide information about cavitation and its effects on membrane permeability, as discussed further in the text.

Table 1. Empirical Correlation of Membrane Permeabilization with Measured Acoustic Signals

	Frequency (kHz)[a]	Correlated equation[b]	r^2 [c]
Set 1a	24 (f)[d]	M = 19.7 ln (P) + 30.6	0.58
	48 (2f)	M = 12.4 ln (P) + 43.2	0.66
	72 (3f)	M = 11.8 ln (P) + 49.2	0.58
	96 (4f)	M = 11.4 ln (P) + 53.6	0.45
Set 1b	23–25 (f)	M = 19.7 ln (P) + 65.0	0.64
	47–49 (2f)	M = 12.7 ln (P) + 64.8	0.70
	71–73 (3f)	M = 12.3 ln (P) + 68.9	0.66
	95–97 (4f)	M = 11.7 ln (P) + 69.4	0.60
Set 2a	12 (f/2)	M = 9.5 ln (P) + 73.0	0.84
	36 (3f/2)	M = 8.5 ln (P) + 64.7	0.85
	60 (5f/2)	M = 8.7 ln (P) + 64.4	0.85
	84 (7f/2)	M = 9.6 ln (P) + 69.6	0.85
Set 2b	11–13 (f/2)	M = 10.1 ln (P) + 79.8	0.81
	35–37 (3f/2)	M = 9.0 ln (P) + 70.8	0.81
	59–61 (5f/2)	M = 9.3 ln (P) + 70.3	0.82
	83–85 (7f/2)	M = 9.8 ln (P) + 73.1	0.82
Set 3	13–23 (b1)	M = 10.2 ln (P) + 82.3	0.75
	25–35 (b2)	M = 10.5 ln (P) + 82.9	0.75
	37–47 (b3)	M = 10.2 ln (P) + 79.5	0.79
	49–59 (b4)	M = 10.6 ln (P) + 80.6	0.78
	61–71 (b5)	M = 10.3 ln (P) + 78.2	0.79
	73–83 (b6)	M = 10.6 ln (P) + 79.7	0.79
	85–95 (b7)	M = 10.2 ln (P) + 77.0	0.78

[a] Based on spectral information such as that shown in Figure 1, membrane permeabilization was correlated with the pressure (or the average pressure when a range of frequencies is given) measured at the frequency (or range of frequencies) indicated.
[b] The equation which resulted from a log-linear fit of membrane permeabilization (M) and measured pressure (P) is shown. There is no mechanistic basis for the log-linear functionality; visual inspection suggested it was the most appropriate fit of the data. The units of permeabilization are percent hemoglobin released and the units of pressure are atm.
[c] The r^2 correlation coefficient is shown for each fit of the data.
[d] The text in parentheses refers to which harmonic of the driving frequency (f = 24 kHz) the indicated frequencies correspond and "b" indicates a broadband noise measurement.

pressure (i.e., < 2.0 atm for degassed water) for the pressure as a function of transducer voltage:

$$P = 0.0089 \cdot V \ (r^2 = 0.99) \quad (1)$$

where peak positive pressure (P) has units of atm and peak-to-peak voltage (V) has units of volts. This equation was extrapolated to higher voltages and pressures and was used to convert measured transducer voltages to the incident pressures reported throughout this study.

Measurement of Ultrasound Power and Heating

In this study, bulk heating caused by ultrasound was measured and determined to be less than 1°C for all exposures. Using an iron/constantan thermocouple (Model SA1-J thermocouple; Model DP 460 display; Omega Engineering, Stamford, CT) inserted into the water bath, which was mixed using a stir bar and magnetic stirrer (VWR), the temperature was determined to rise at 0.17°C/min during continuous exposure to ultrasound at 2.2 atm and 0.73°C/min at 4.5 atm incident pressure.

Although we have reported incident pressure rather than power to characterize the strength of ultrasound, it may be helpful for comparison with other studies to know the power of ultrasound exposures used here. Assuming that all acoustic energy from the transducer was eventually converted into heat and heat loss from the apparatus to the surroundings was negligible, the measured heating rates described above can be used to determine the power output of the transducer with the equation

$$W = m_{water} C_{p_{water}} dT/dt \quad (2)$$

where W is power, m_{water} is the mass of water in the water bath (0.3 kg), $C_{p_{water}}$ is the heat capacity of water (4.18 J/g°C (21)), and dT/dt is the change of temperature with respect to time (e.g., 0.17°C/min at 2.2 atm). For example, using the heating rates given above this yields 3.4 W at 2.2 atm and 15.1 W at 4.5 atm. This type of calorimetric method is commonly used to estimate ultrasonic power (22).

A second method to determine the power of ultrasound exposures was to measure the electrical power supplied to the transducer. The values determined by the two methods should be equal if there is complete conversion of electrical power to acoustic power by the transducer (i.e., 100% efficiency). The voltage across the transducer was measured directly with an oscilloscope (model 2430A, Tektronics, Beaverton, OR) and the current was measured using a current transformer (Model 2100, Pearson Electronics, Palo Alto, CA) and fed to the oscilloscope. The average power was calculated as the average of the product of the current and voltage signals and yielded the following relationship

$$W = 0.00010 \cdot V^2 \ (r^2 = 1.00) \quad (3)$$

where power (W) has units of watts and peak-to-peak voltage (V) has units of volts. Combination of equations (1) and (3) yields an equation which relates power to incident pressure for the experimental apparatus used in this study:

$$W = 1.3 \cdot P^2 \quad (4)$$

where power (W) has units of watts and incident pressure (P) has units of atm. This equation indicates the power to be 6.3 W at 2.2 atm and 26 W at 4.5 atm. The values determined using equation (4) are considerably higher than those determined using equation (2). This is expected since equation (4) assumes 100% efficient conversion of electrical energy by the transducer into acoustic energy, which should yield an overprediction. In contrast, equation (2) assumes perfect insulation of the apparatus, which should yield an underprediction. Thus, equations (2) and (4) provide upper and lower bounds for the acoustic energy.

Post-Exposure Analysis

After exposure to ultrasound, samples were removed from the sample tube and spun down (as above). The supernatant contained free hemoglobin released from permeabilized cells, while the pellet contained intact cells. The supernatant was collected and the absorbance of hemoglobin in the supernatant was determined at 575 nm using a spectrophotometer (DU-64, Beckman Instruments). As a positive control, the absorbance was also determined for a sample in which all cells were lysed by suspension in deionized water. The ratio of these absorbances yielded the percent hemoglobin released, expressed as percent membrane permeabilization in the figures.

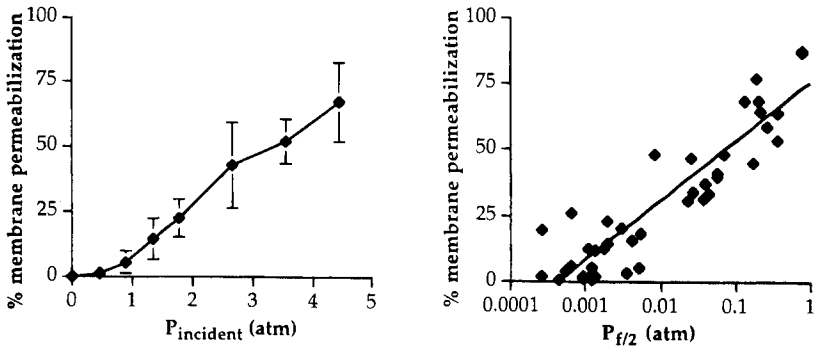

Fig. 2. The effect of ultrasonic pressure on membrane permeabilization by ultrasound. A suspension of bovine red blood cells was exposed to continuous ultrasound for 10 sec at 24 kHz. The degree of membrane permeabilization was assessed by release of hemoglobin. Permeabilization increased with increasing (A) incident pressure (f = 24 kHz), a measure of the total ultrasound exposure which cannot be measured directly in the presence of cavitation, and (B) subharmonic pressure (f/2 = 12 kHz), a measure of cavitation which can be measured directly. This figure suggests that membrane permeabilization is mediated by cavitation and that measurement of subharmonic pressure may be a noninvasive way to determine the degree of permeabilization, and thereby the amount of drug delivery, resulting from ultrasound exposure. See text for discussion.

RESULTS

To develop a rational approach to designing protocols for ultrasound-mediated cell membrane permeabilization, we measured the degree of permeabilization of bovine red blood cells exposed to low-frequency (24 kHz) ultrasound as a function of incident ultrasound pressure, total exposure time, pulse length, and duty cycle. In addition, we correlated the amount of permeabilization with measurable acoustic signals, which is of interest to noninvasive monitoring of ultrasound's bioeffects and elucidation of mechanisms. The degree of permeabilization was measured by release of hemoglobin from erythrocytes.

Figure 2a shows the dependence of red blood cell permeabilization on the incident pressure of ultrasound. Permeabilization increased with incident pressure, exhibiting an almost linear dependence for pressures greater than ~0.5 atm. This is consistent with previous studies which show that bioeffects increase with ultrasound pressure or intensity (14–17).

For pharmaceutical applications, it would be helpful to noninvasively determine the effects of ultrasound on cells based on an acoustic measurement. In this way, intelligent drug delivery systems could receive real-time feedback about membrane permeabilization and resultant drug uptake by simply "listening." Figure 1b shows a representative spectrum of acoustic signals associated with an ultrasound exposure which causes extensive cavitation. A strong signal is seen at the driving frequency, f (i.e., 24 kHz), which is the frequency at which the transducer resonates. Due to cavitation and other effects there are also strong signals at integer multiples of the driving frequency (i.e., 2f, 3f, 4f) and at the subharmonic frequency, f/2, and its ultraharmonics (i.e., 3f/2, 5f/2, 7f/2). The broadband noise pressure between these peaks (i.e., b1, b2, etc.) is also elevated.

We assessed whether cell membrane permeabilization correlates with any of these features of the acoustic spectrum, as summarized in Table 1. The correlation was strongest for $P_{f/2}$ (i.e., the pressure at f/2) and its ultraharmonics (set 2). Figure 2b shows this relationship graphically. Permeabilization also correlated with average measurements of broadband noise pressure between the peaks (set 3). The driving frequency itself and its higher harmonics (set 1) showed the weakest correlation. Previous studies have correlated cell damage with $P_{f/2}$ (23) and 20 f (24). Mechanistic interpretation of these results is discussed below. These correlations may provide a useful means for noninvasively measuring cell permeabilization by ultrasound.

The effect of total exposure time of a single continuous ultrasound exposure is shown in Figure 3. Below approximately 100 msec, ultrasound had little effect on the cells. For longer exposures, membrane permeabilization increased as a strong function of exposure time. This is in qualitative agreement with previous studies conducted under somewhat different conditions, which also show that membrane disruption increases with exposure time above a threshold (25,26).

In Figure 4, cells were exposed to ultrasound using pulses of different length, but the cumulative "on" time for each set of pulses was kept constant at 10 sec. For each pressure tested, the degree of membrane permeabilization varied little as a

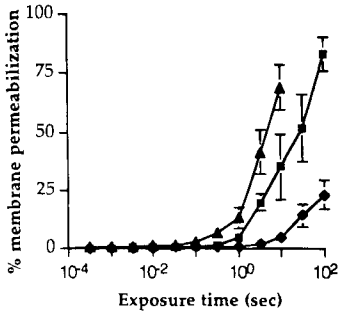

Fig. 3. The effect of exposure time on membrane permeabilization by ultrasound. Red blood cells were exposed to continuous ultrasound at 24 kHz for different amounts of time at three different incident pressures: (♦) 0.89 atm, (■) 2.7 atm, (▲) 8.9 atm. In each case, permeabilization increased with exposure time above a threshold of approximately 100 msec.

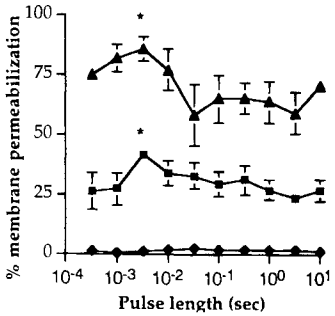

Fig. 4. The effect of ultrasound pulse length on membrane permeabilization. In each exposure, although pulses of different length were applied, the total number of pulses given was varied so that the cumulative "on" time was kept constant at 10 sec. Pulses were applied at a duty cycle of 10% and at three different incident pressures: (♦) 0.89 atm, (■) 2.7 atm, (▲) 8.9 atm. Permeabilization showed a weak dependence on pulse length, with a small but statistically significant peak at 3 msec for both 2.7 and 8.9 atm ($p < 0.05$, by Student's T-test, relative to average permeabilization at pulse lengths $\geq$ 0.1 sec).

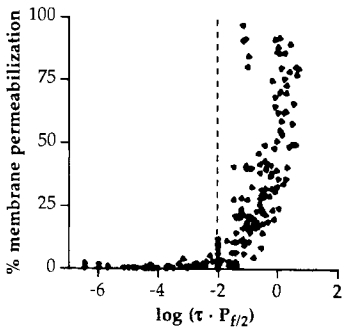

Fig. 6. Membrane permeabilization shown as a fuction of the measurable acoustic parameter $\tau \cdot P_{f/2}$. This figure includes all 252 data points from this study (i.e., Figures 2–5). The parameter $\tau \cdot P_{f/2}$ was chosen because it characterizes the total cavitational exposure by accounting for both the strength of the f/2 cavitation signal ($P_{f/2}$) and the time over which it acts (τ). The good correlation between permeabilization and $\tau \cdot P_{f/2}$ is significant because measurement of this single parameter may provide a simple, non-invasive method for determining membrane permeabilization caused by any ultrasound exposure.

function of pulse length. There was, however, a small statistically-significant peak in permeabilization at 3 msec. A possible physical explanation for this peak is discussed below.

For pulsed ultrasound, the effect of duty cycle (defined as the fraction of time that the ultrasound is "on" during pulsed application) is shown in Figure 5. Under the conditions investigated, duty cycle had no significant effect on the degree of membrane permeabilization.

Figure 2b shows that $P_{f/2}$ is predictive of the degree of membrane permeabilization from exposures of different incident pressure but all having the same pulse length, exposure time and duty cycle. To generalize the approach and consider exposures of different pulse lengths, exposure times, duty cycles and incident pressures, we correlated membrane permeabilization with the total exposure time (τ), which is equal to the product of pulse length and the number of pulses applied, multiplied by the strength of the f/2 signal ($P_{f/2}$). As shown in Figure 6, this parameter ($\tau \cdot P_{f/2}$) correlated well with membrane permeabilization, showing a threshold value at approximately 0.01 (i.e., $\log(\tau \cdot P_{f/2}) = -2$). Below this threshold little permeabilization occurred and above it permeabilization increased sharply. Because Figure 6 includes all of the data collected in this study and because the parameter $\tau \cdot P_{f/2}$ correlates well with the whole data set, this suggests that measurement of this single parameter may provide a simple, non-invasive and broadly-applicable method for determining membrane permeabilization caused by any ultrasound exposure. Additional tests using different ultrasound frequencies, apparatus geometries, and cell/tissue types are needed to verify this hypothesis.

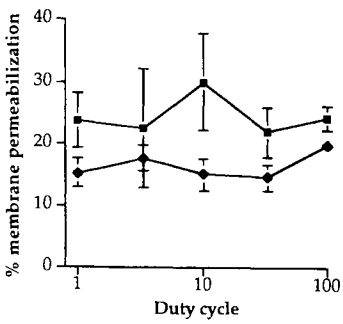

Fig. 5. The effect of ultrasound duty cycle on membrane permeabilization. Duty cycle is defined as the fraction of time that the ultrasound is "on" during pulsed application. In each exposure, the incident pressure was 2.7 atm, the total "on" time was 10 sec, and the pulse length was (♦) 0.1 sec or (■) 1 sec. Permeabilization showed no statistically-significant dependence on duty cycle.

DISCUSSIONS

Effect of Ultrasound Parameters

Characterizing the dependence of cell membrane permeabilization on ultrasound conditions is essential to rationally designing ultrasound protocols for pharmaceutical application. This study shows that permeabilization increases as a strong function of incident pressure (Figure 2) and total exposure time (Figure 3), which indicates that selection of appropriate pressure and duration of ultrasound exposure is important to achieve permeabilization at a desired level. The existence of a threshold near 100 msec of total exposure time (Figure 3) also constrains possible protocols. In contrast, the observation that permeabilization depends only weakly on pulse length (Figure 4) and duty cycle (Figure 5) is useful information, since it permits greater flexibility in designing ultrasound protocols.

The effects of different ultrasound parameters summarized above can be explained in terms of cavitation, the mechanism by which membranes are believed to be disrupted (16,19). It is well established that at greater acoustic pressure more cavitation bubbles with greater energy are created (19). Similarly, longer total exposure times also yield more cavitation bubbles. This increased cavitation should result in more extensive membrane permeabilization, as seen in Figures 2 and 3. The minimum exposure time of 100 msec shown in Figure 3 could result from the "warm-up" time it takes for bubbles to nucleate, grow, and possibly collapse over many ultrasound cycles (27).

The maximum permeabilization observed for 3 msec pulses in Figure 4 could be explained by two competing effects

involving a mechanism proposed previously (28). Increasing pulse length is advantageous for cavitation because there is more time during each pulse for bubbles to nucleate, grow and collapse. However, as pulse length increases so does the time between pulses at constant duty cycle. This means that as the interpulse delay increases, bubbles formed during the previous pulse have time to dissolve back into solution. This is disadvantageous because it leaves fewer nucleation bubbles available to grow and collapse during the next pulse, which results in less cavitation. Further experiments are required to verify this hypothesis.

Correlation with Measured Acoustic Signals

Ultrasound causes cavitation which in turn causes effects on cells. Therefore the most useful predictor of ultrasound's effects on cells should be a measure of cavitation. We correlated membrane permeabilization with measured acoustic signals which are known to be associated with cavitation. A good correlation was found for the pressure measured at half the driving frequency (f/2 = 12 kHz) and its ultraharmonics (Figure 2b, set 2 of Table 1). In addition, permeabilization caused by ultrasound applied at any set of conditions tested in this study could be well predicted by the parameter $\tau \cdot P_{f/2}$, which characterizes the total cavitational exposure by accounting for both the strength of the f/2 cavitation signal and the time over which it acts. Although validation of this idea requires further testing, these findings suggest that a device could apply ultrasound to a tissue, such as skin or a tumor, and by measuring the f/2 signal assess the degree to which the tissue was permeabilized. This information could then be used to estimate the amount of drug delivered. In this way, measurement of the f/2 signal could potentially provide a method for real-time feedback so that a device could optimize the ultrasound exposure based on preprogrammed or user-selected drug delivery profiles. The technology required for both generating ultrasound and "listening" to f/2 signals are well established, relatively inexpensive when mass produced, and readily miniaturizable.

Correlation of acoustic signals with membrane permeabilization also provides mechanistic insight. The best correlation was found for the signal at f/2 and its ultraharmonics (set 2 of Table 1, Figure 2b). This suggests that permeabilization was mediated by cavitation. Onset of the f/2 signals is thought to occur with the onset of cavitation (19). As the cavitation activity increases, the f/2 signals also generally increase, but a quantitative relationship between amount of cavitation and $P_{f/2}$ has not been established. Cavitation bubbles are thought to give off a signal at f/2 because of a prolonged expansion phase and delayed collapse which can occur during cavitation (19). In our experiments, measurement of f/2 signals at the exact frequency of interest (e.g., 12 kHz; set 2a) yielded a somewhat better correlation with permeabilization than measurement of the signal over the width of the peak (e.g., 11–13 kHz; set 2b).

A reasonable correlation was also established for measurements of broadband signals, or the signals between f, f/2, and higher harmonics (set 3 of Table 1). This also supports a permeabilization mechanism involving cavitation, especially transient cavitation. Upon bubble collapse during transient cavitation, "noise" over a broad spectrum of frequencies is given off, which raises peak and broadband signals alike (19). Since both f/2 and broadband signals showed correlation, this suggests that both stable and transient cavitation play a role in membrane permeabilization.

Finally, signals at f and its higher harmonics showed the poorest correlation (set 1 in Table 1). This was expected since these signals are related to the non-cavitational driving frequency (f) and resonance of the experimental apparatus (higher harmonics), in addition to stable and transient cavitation. As a signal which reflects a mixture of effects, f and its higher harmonics would not be expected to be good indicators.

CONCLUSIONS

While ultrasound-mediated cell membrane permeabilization is a promising new method for enhanced and targeted drug delivery, the dependence of permeabilization on acoustic parameters has not been sufficiently defined for pharmaceutical applications. Using red blood cells as a model system, we showed that membrane permeabilization increases with incident ultrasound pressure, increases with total exposure time above a threshold of 100 msec, shows a weak dependence on pulse length with a small maximum at 3 msec, and does not depend on duty cycle under the conditions examined. In addition, the degree of permeabilization was shown to correlate with measurable acoustic signals (e.g., $P_{f/2}$, $\tau \cdot P_{f/2}$), which supports the hypothesis that permeabilization is mediated by cavitation and may provide a method for noninvasive, real-time feedback for an intelligent delivery system.

ACKNOWLEDGMENTS

We thank Keyvan Keyhani, Hector Guzman, Aimee Parsons, Joanne Farrell, and Samir Mitragotri for helpful discussions. This work was supported in part by an NSF Career Young Investigator Award (BES-9624832), the Hoechst-Celanese Corporation, The Whitaker Foundation, and the Frank H. Neely Endowment at Georgia Tech.

REFERENCES

1. A. R. Williams. A possible alteration in the permeability of ascites cell membranes after exposure to acoustic microstreaming. *J. Cell Sci.* **12**:875–885 (1973).
2. A. H. Saad and G. M. Hahn. Ultrasound-enhanced effects of adriamycin against murine tumors. *Ultrasound Med. Biol.* **18**:715–723 (1992).
3. M. Fechheimer, J. F. Boylan, S. Parker, J. E. Sisken, F. L. Patel, and S. G. Zimmer. Transfection of mammalian cells with plasmid DNA by scrape loading and sonication loading. *Proc. Natl. Acad. Sci. USA* **84**:8463–8467 (1987).
4. H. J. Kim, J. F. Greenleaf, R. R. Kinnick, J. T. Bronk, and M. E. Bolander. Ultrasound-mediated transfection of mammalian cells. *Human Gene Ther.* **7**:1339–1346 (1996).
5. S. Bao, B. D. Thrall, and D. L. Miller. Transfection of a reporter plasmid into cultured cells by sonoporation in vitro. *Ultrasound Med. Biol.* **23**:953–959 (1997).
6. J. A. Wyber, J. Andrews, and A. D'Emanuele. The use of sonication for the efficient delivery of plasmid DNA into cells. *Pharm. Res.* **14**:750–756 (1997).
7. L.-J. Zhang, L.-M. Cheng, N. Xu, N.-M. Zhao, C.-G. Li, J. Yuan, and S.-R. Jia. Efficient transformation of tobacco by ultrasonication, *Bio/Technology* **9**:996–997 (1991).
8. R. P. Holmes, L. D. Yeaman, R. G. Taylor, and D. L. McCullough. Altered neutrophil permeability following shock wave exposure in vitro. *J. Urol.* **147**:733–737 (1992).
9. S. Gambihler, M. Delius, and J. W. Ellwart. Permeabilization of the plasma membrane of L1210 mouse leukemia cells using lithotripter shock waves. *J. Membr. Biol.* **141**:267–275 (1994).

10. J. Kost and R. Langer. Ultrasound-mediated transdermal drug delivery. In V. P. Shah and H. I. Maibach (eds.), *Topical Drug Bioavailability, Bioequivalence, and Penetration,* Plenum Press, New York, 1993, pp. 91–104.
11. S. Mitragotri, D. Blankschtein, and R. Langer. Transdermal drug delivery using low-frequency sonophoresis. *Pharm. Res.* **13**:411–420 (1996).
12. S. Mitragotri, D. Blankschtein, and R. Langer. Ultrasound-mediated transdermal protein delivery. *Science* **269**:850–853 (1995).
13. M. R. Prausnitz. Reversible skin permeabilization for transdermal delivery of macromolecules. *Crit. Rev. Ther. Drug Carrier Syst.* **14**:455–483 (1997).
14. H. F. Stewart and M. E. Stratmeyer (eds.). *An Overview of Ultrasound: Theory, Measurement, Medical Applications, and Biological Effects (FDA 82-8190),* U.S. Department of Health and Human Services, Rockville, MD, 1983.
15. K. S. Suslick (ed.). *Ultrasound: Its Chemical, Physical, and Biological Effects,* VCH, Deerfield Beach, FL, 1988.
16. S. B. Barnett, G. R. ter Haar, M. C. Ziskin, W. L. Nyborg, K. Maeda, and J. Bang. Current status of research on biophysical effects of ultrasound. *Ultrasound Med. Biol.* **20**:205–218 (1994).
17. NCRP. *Exposure Criteria for Medical Diagnostic Ultrasound: I. Criteria Based on Thermal Mechanisms (NCRP Report No. 113),* National Council on Radiation Protection and Measurements, Bethesda, MD, 1992.
18. A. J. Coleman and J. E. Saunders. A review of the physical properties and biological effects of the high amplitude acoustic fields used in extracorporeal lithotripsy. *Ultrasonics* **31**:75–89 (1993).
19. T. G. Leighton. *The Acoustic Bubble,* Academic Press, London, 1994.
20. T. J. Matula, R. A. Roy, and P. D. Mourad. Optical pulse width measurements of sonoluminscence in cavitation-bubble fields. *J. Acoust. Soc. Am.* **101**:1994–2002 (1997).
21. R. C. Weast (ed.). *CRC Handbook of Chemistry and Physics,* CRC Press, Boca Raton, FL, 1985.
22. T. Kimura, T. Sakamoto, J. -M. Leveque, H. Sohmiya, M. Fujita, S. Ikeda, and T. Ando. Standardization of ultrasonic power for sonochemical reaction. *Ultrasonics Sonochem.* **3**:S157–S161 (1996).
23. R. J. Jeffers, R. Q. Feng, J. B. Fowlkes, J. W. Hunt, D. Kessel, and C. A. Cain. Dimethylformamide as an enhancer of cavitation-induced cell lysis in vitro. *J. Acoust. Soc. Am.* **97**:669–676 (1995).
24. E. C. Everbach, I. Raj, S. Makin, M. Azadniv, and R. S. Meltzer. Correlation of ultrasound- induced hemolysis with cavitation detector output in vitro. *Ultrasound Med. Biol.* **23**:619–624 (1997).
25. L. O. Kober, J. W. Ellwart, and H. Brettel. Effect of the pulse length of ultrasound on cell membrane damage in vitro. *J. Acoust. Soc. Am.* **86**:6–7 (1989).
26. A. A. Brayman, M. Azadniv, C. Cox, and M. W. Miller. Hemolysis of albunex-supplemented, 40% hematocrit human erythrocytes in vitro by 1-MHz pulsed ultrasound: acoustic pressure and pulse length dependence. *Ultrasound Med. Biol.* **22**:927–938 (1996).
27. M. A. Margulis. Kinetics of the number of cavitation bubbles in an ultrasonic field. *Sov. Phys. Acoust.* **22**:145–147 (1976).
28. V. Ciaravino, H. G. Flynn, and M. W. Miller. Pulsed enhancement of acoustic cavitation: a postulated model. *Ultrasound Med. Biol.* **7**:159–166 (1981).